

Continual Learning for Multimodal Data Fusion of a Soft Gripper

Nilay Kushawaha^{a,b,*}, Egidio Falotico^{a,b}

^aThe BioRobotics Institute, Scuola Superiore Sant'Anna, Pontedera, Italy

^bDepartment of Excellence in Robotics and AI, Scuola Superiore Sant'Anna, Pisa, Italy

ARTICLE INFO

Keywords:

Continual Learning
Semi-supervised learning
Multimodality
Robot operating system
Class prototypes

ABSTRACT

Continual learning (CL) refers to the ability of an algorithm to continuously and incrementally acquire new knowledge from its environment while retaining previously learned information. A model trained on one data modality often fails when tested with a different modality. A straightforward approach might be to fuse the two modalities by concatenating their features and training the model on the fused data. However, this requires retraining the model from scratch each time it encounters a new domain. In this paper, we introduce a continual learning algorithm capable of incrementally learning different data modalities by leveraging both class-incremental and domain-incremental learning scenarios in an artificial environment where labeled data is scarce, yet non-iid (independent and identical distribution) unlabeled data from the environment is plentiful. The proposed algorithm is efficient and only requires storing prototypes for each class. We evaluate the algorithm's effectiveness on a challenging custom multimodal dataset comprising of tactile data from a soft pneumatic gripper, and visual data from non-stationary images of objects extracted from video sequences. Additionally, we conduct an ablation study on the custom dataset and the Core50 dataset to highlight the contributions of different components of the algorithm. To further demonstrate the robustness of the algorithm, we perform a real-time experiment for object classification using the soft gripper and an external independent camera setup, all synchronized with the Robot Operating System (ROS) framework.

1. Introduction

In recent years, machine learning models have matched or even exceeded human-level performance on tasks such as image classification Ahmad et al., object recognition Zou et al., natural language processing (NLP) Otter et al., playing games in simulation, etc. While these models excel in static tasks where the data distribution remains constant, they encounter difficulties in adapting to changing environments and need to restart the training process whenever new data is introduced. On the other hand, humans are adept at learning from dynamic environments, continuously acquiring, updating, and applying knowledge over time. We expect AI systems to adapt in a similar fashion.

Continual learning (CL) Wang et al., Lesort et al., also known as lifelong learning or incremental learning, is a machine learning subfield that focuses on progressively training models on a continuous stream of data to accumulate and retain knowledge over time. However, a significant obstacle for these artificial models is their tendency to forget previously acquired skills when exposed to new tasks or data distributions. This issue, known as catastrophic forgetting, often leads to a substantial drop in performance as the new information overwrites the old knowledge or alters the data distribution. A naive solution to this problem is to save all data, shuffle it, and retrain the model offline from scratch. While this method effectively addresses catastrophic forgetting, it is time-inefficient, suboptimal, and unsustainable for modern large-scale models that require significant computational power. Continual learning aims to develop methods

that balance performance and efficiency more effectively. Robots operating in unstructured real world environments will encounter new tasks and challenges over time, necessitating capabilities that cannot be fully anticipated from the outset. These robots need to learn continually, acquiring new skills without forgetting previously learned ones.

A model trained in one domain will be ineffective when deployed in a completely different domain or used with a different data modality than it was originally trained on. One straightforward approach might be to use separate models for each data modality or to jointly train a single model on all modalities offline. However, this is not a feasible solution for agents with limited memory and computational resources that learns new domains through active exploration and interaction with its environment. Another challenge is the limited availability of labeled data for supervised incremental training. A large research effort is dedicated towards learning from unlabeled data, which is often more readily available than labeled data in practical applications. Within this effort, the field of semi-supervised learning (SSL) Van Engelen and Hoos has recently demonstrated the most promising results. In this setting, an agent can utilize a significant amount of unlabeled data from its environment. It can employ the knowledge gained from labeled data to learn new objects of the same class or to enrich its understanding of previously learned classes using the unlabeled data.

In this paper, we consider a realistic continual learning problem where a single continual learning model learns different modalities of data incrementally by leveraging both class-incremental and domain-incremental learning scenarios in an artificial environment where labeled data is scarce yet non-iid (independent and identical distribution) unlabeled data from the environment is plentiful. We mainly experiment with two different SSL conditions: *Radom images*,

*Corresponding author

 nilay.kushawaha@santannapisa.it (N. Kushawaha);

egidio.falotico@santannapisa.it (E. Falotico)

ORCID(s): 0000-0003-2416-9794 (N. Kushawaha); 0000-0001-8060-8080 (E. Falotico)

where for each object of the same parent class we randomly sample some images from the dataset that are not included in the training data; *Unique objects*, where we sample the images of new unseen objects that belong to the same parent class. More details about the SSL conditions is provided in section 3.3.

To perform a multimodal CL experiment, we leverage two different modalities of data mainly the tactile data coming from sensors integrated with a soft gripper and the visual data from an independent camera setup. The CL model is designed to learn the classes in both the domains incrementally. To address this issue of multimodal CL, we build on the feature covariance-aware metric (FeCAM) algorithm by Goswami et al. and propose an extended version of the algorithm that employs an incremental online semi-supervised learning process for each task. We call it exFeCAM or extended FeCAM algorithm. Additionally, our algorithm includes an intra-layer feature representation mechanism to learn more generalized feature maps for each class. To the best of our knowledge, we are the first to use a continual learning model in a multimodal data setting where an agent learns both tactile data and vision data provided by respective sensors. The main contributions of this article are summarized as follows:

1. We present an online non-exemplar continual learning algorithm with SSL capabilities. In addition, to enhance the feature maps from the pre-trained layers, we introduce intra-layer feature representations.
2. We present a new multimodal non-iid dataset for real world continual learning applications.
3. We demonstrate the robustness of learning different modalities as a new incremental domain rather than just combining the data from different modalities into a single fused feature vector.
4. We evaluate our algorithm on the custom multimodal dataset as well as the Core50 dataset Lomonaco and Maltoni and perform an ablation study to verify the effectiveness of the various parts of the algorithm.
5. We also perform a real-time experiment for object classification on the soft pneumatic gripper equipped with sensors and a separate camera setup, all synchronised using the ROS framework Koubaa et al.. More details about the experiment is provided in section 6.

The paper is structured as follows: In Section 2, an overview of the related works in CL, SSL, and multimodality is presented, with a focus on the recent advancements in the literature. Section 3 provides a detailed description of the experimental setup that has been adopted discussing the different cl strategies, data accumulation steps, and evaluation metrics. Following this, the proposed methodology is presented in Section 4, which includes the model architecture and the framework used in this study. The evaluation of the proposed methodology on custom multimodality dataset, as well as the Core50 dataset is provided in section 5. Moreover, in section 6 the paper showcases the real-time application of the proposed algorithm. Finally, a summary

noting the advantages and disadvantages of the proposed method along with the scope for improvements and possible developments in the future are stated in the last section.

2. Related Work

2.1. Continual Learning Strategies

Continual learning strategies can be broadly categorized into four major types: architectural, regularization, rehearsal, and hybrid strategies, each with its own advantages and disadvantages. Architectural strategy either employs a dynamic modular network where new layers gets added upon encounter of new tasks Rusu et al., Fernando et al., Rajasegaran et al., Aljundi et al. or performs parameter isolation to allocate a dedicated separate sub-space for each task within the same network Mallya et al., Serra et al., Mallya and Lazebnik, Ahn et al.. The simplest form of architectural regularization involves freezing certain weights in the network to ensure they remain unchanged during training on new tasks. A major drawback of the architectural strategy is the increase in the size of the architecture as new tasks are learned or the potential saturation of the architecture if a fixed model is used.

Regularization strategies can be grouped into two: weight regularization and function regularization. Weight regularization constrains the update of the network weights by adding explicit regularization terms to the loss function, penalizing changes in each parameter based on its importance Kirkpatrick et al., Zenke et al., Chaudhry et al., Aljundi et al.. Function regularization, on the other hand, employs distillation methods to maintain the knowledge between the various layers of the network. This strategy typically employs the previously-learned model as the teacher and the currently model as the student, while implementing knowledge distillation (KD) techniques Hinton et al., Li and Hoiem, Rebuffi et al. Dhar et al., Lee et al.. However, regularising the model can make it more challenging for the network to acquire new knowledge.

Rehearsal Lopez-Paz and Ranzato, Bang et al., Kumari et al., Ebrahimi et al., Saha and Roy & pseudo-rehearsal, Shin et al., Wu et al., Ayub and Wagner, Pfülb and Gepperth, Wang et al. approaches offer the most simple yet effective approach by storing a subset of the previously learned data in a memory buffer or by training a generative model to account for the previous information and replaying it during training on new tasks. However, storing the images in a replay buffer for rehearsal can raise privacy concerns. On the other hand, while using a generative model somewhat addresses the privacy issues but may result in increased training time and computational demands.

Hybrid strategies Van de Ven et al., Liu et al., Ye and Bors are a combination of any of the other three strategies to compensate for catastrophic forgetting. SynapNet Kushawaha et al. uses a triple model architecture incorporating knowledge distillation along with a VAE-based pseudo-episodic memory for rehearsal and a sleep phase for memory re-organization. DualNet Pham et al. uses a fast learner for

supervised learning and a slow learner for unsupervised learning of task-agnostic general representation using semi-supervised learning. ICARL Rebuffi et al. includes an external fixed memory to store a subset of old task data based on an elaborated sample selection procedure and then employs a distillation step acting as a regularization.

Non-exemplar continual learning strategies Goswami et al., Petit et al., Smith et al., Hayes et al. use the idea of replay-free sequential training, instead of using a modular network or regularizing the optimization function. Exemplar-free approaches store the prototypes of the past and new classes to compensate for catastrophic forgetting of the previously acquired knowledge. A pre-trained feature extractor provides the feature maps which are then used to calculate the mean and the covariance matrix for the respective classes.

2.2. Semi-Supervised Learning

Semi-supervised learning describes a class of algorithms designed to learn from both labeled and unlabeled data, typically assumed to be sampled from the same or similar distributions Yan et al., Mawuli et al.. One of the critical challenges in semi-supervised learning is how to effectively utilize labeled and unlabeled data while avoiding overfitting, preventing the effects of noise on the model, and ensuring effective model performance enhancement. Initial breakthroughs in semi-supervised learning with deep neural networks leveraged generative models such as autoencoders Rasmus et al., variational autoencoders Kingma et al., and generative adversarial networks Odena.

Some approaches in semi-supervised learning Oliver et al., Berthelot et al., Lee et al., Kingma et al., Kuo et al. also involve balancing a supervised loss (l_s) applied to the labeled data and an unsupervised consistency regularization loss l_{ul} computed on the unlabeled data. Consistency regularization aims to improve model resilience and maintain label distribution, even in the presence of noisy images. It measures the discrepancy between predictions made on perturbed unlabeled data points. Approaches of this kind include the π -model Laine and Aila which augments the input data with image-based noise and self-regularizes through an additional consistency loss, mean teacher Tarvainen and Valpola, which employs an exponential moving average of parameters to regularize the model. Recently, fast-SWA Athiwaratkun et al. showed improved results by training with cyclic learning rates and measuring discrepancy with an ensemble of predictions from multiple checkpoints.

Two additional important approaches for semi-supervised learning, which have shown success both in the context of deep neural networks and other types of models are: self-training and conditional entropy minimization. Self-training also known as pseudo-labeling Lee et al. involves assigning classes to unlabeled data by making predictions from a model trained only on labeled data. Furthermore, co-training Xie et al. attempts to analyze data from different perspectives to solve the accumulative mistake issue during self-training. On the other hand, in case of conditional

entropy minimization Grandvalet and Bengio, all unlabeled examples are encouraged to make confident predictions on some class. This doesn't necessarily mean the predictions are correct (because the true labels for the unlabeled data are unknown), but the model is incentivized to be decisive rather than uncertain. In this paper, we use the concept of cosine similarity between labeled and unlabeled feature representations for pseudo-labeling of the unsupervised data. We refer to Van Engelen and Hoos for a comprehensive review on the topic.

2.3. Multimodality

Our experience of the world is inherently multimodal we perceive objects through vision, hear sounds, feel textures, smell odors, and taste flavors. To develop an AI agent with similar capabilities, researchers have explored various methods Donato et al., Babadian et al..

The simplest method to compensate multiple domains is using the concept of joint representation where the unimodal signals are combined in the same representation space by simple concatenation Baltrušaitis et al.. Ngiam et al. used autoencoders for multimodal domains. They employed stacked denoising autoencoders to represent each modality individually and subsequently fusing them into a unified multimodal representation using an additional autoencoder layer.

Similarly, Silberer and Lapata suggested a multimodal autoencoder for semantic concept grounding. They incorporated a reconstruction loss for training the representation and added a term in the loss function to predict object labels using the representation. Srivastava and Salakhutdinov introduced multimodal deep belief networks (DBNs) and multimodal deep boltzmann machines (DBMs) Srivastava and Salakhutdinov as multimodal representations. Kim et al. used a deep belief network for each modality and then combined them into joint representation for audiovisual emotion recognition. Huang and Kingsbury used a similar model for audio-visual speech recognition (AVSR), and Wu and Shao used it for audio and skeleton joint based gesture recognition. Ouyang et al. explored the use of multimodal DBMs for the task of human pose estimation from multi-view data. They demonstrated that integrating the data at a later stage after unimodal data, underwent nonlinear transformations, which was beneficial for the model. An alternative to a joint multimodal representation is a coordinated representation where instead of projecting the modalities together into a joint space, separate latent representations are learned for each modality and are coordinated through a constraint Frome et al..

Sarfraz et al. recently utilized a multimodal CL dataset to learn complementary information from two different modalities. They employed the VGGSound dataset, which includes 10-second video clips along with their corresponding audio. On the other hand, Xu et al. developed an egocentric multimodal dataset using smart glasses equipped with sensors, combining data from cameras, accelerometers, and gyroscopes. This dataset covers 32 types of daily activities

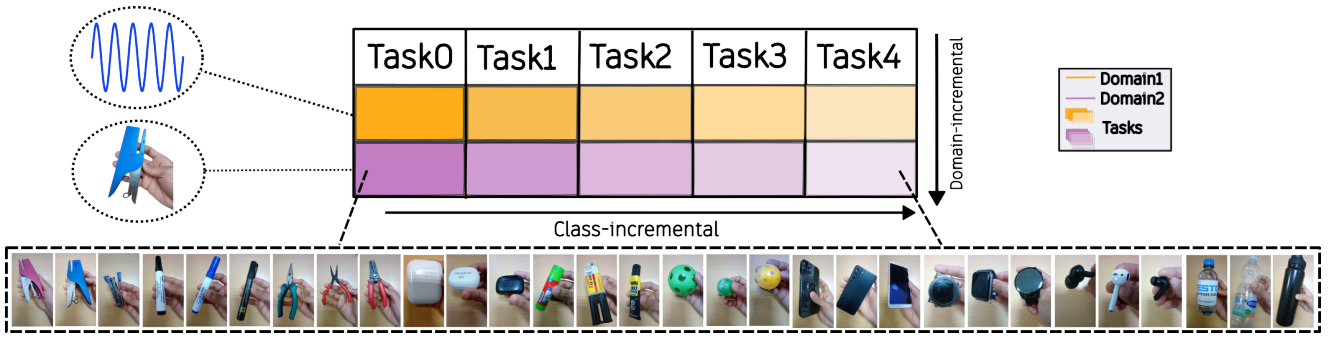


Figure 1: Multimodal data comprising of two different domains, domain 1 contains the sensor information for different objects and domain 2 contains the images of those objects in different orientations, lighting conditions and different level of occlusion by the operator. Moving from left to right the model trains in a class-incremental manner, while going from top-bottom it trains in a domain-incremental manner.

performed by 10 participants. They utilized the temporal binding network (TBN) Kazakos et al. to fuse the information from different sensors into single feature vector for further training and feature extraction.

One of the major drawbacks of these methods is their inability to incrementally learn new domains. For example, if we train our model on two domains (sensor signals and images) and use a joint representation to learn these two modalities, introducing a new data modality later would necessitate re-training the model from scratch. Conversely, with our proposed exFeCAM model, we can add the new modality as a different domain and incrementally train the model without starting the training process anew. Additionally, our algorithm eliminates the necessity of storing data in memory for rehearsal, effectively addressing privacy concerns and storage challenges commonly encountered in exemplar-based CL methods.

With recent advancements in large language models (LLMs) and the introduction of GPT-4 Achiam et al. and its variants, it is now possible to utilize the data coming from vision, audio, and text signals into a single model. However, these models face significant challenges, including high computational and memory demands and a lack of continual learning capabilities.

3. Experimental Setup

In this section, we describe the steps involved in the creation of the multimodal continual learning dataset as well as the standard evaluation criteria for the class incremental as well as domain incremental learning scenarios.

3.1. Continual Learning Scenario

According to the division of incremental batches and the availability of task identities, continual learning can be broadly classified into three primary types or scenarios Van de Ven et al.:

- **Task-Incremental Learning (TIL):** It requires an algorithm to learn a set of distinct tasks progressively. Task

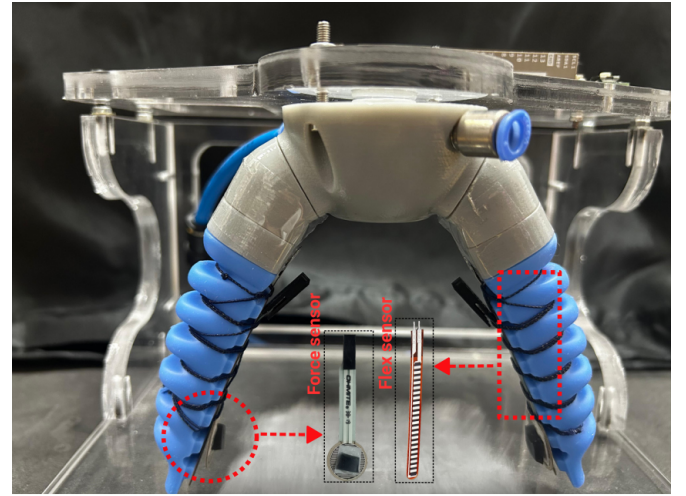


Figure 2: Commercial two fingers pneumatic gripper equipped with two force sensors and two flex sensors affixed together using stretchable nylon thread. The flex sensor measures the bending of the finger and the force sensor measures the magnitude of the force applied to the finger tip.

identities/numbers are provided in both training and testing phase.

- **Class-Incremental Learning (CIL):** The algorithm must learn to differentiate between a growing number of classes incrementally. Task identities are only provided during training phase.
- **Domain-Incremental Learning (DIL):** The algorithm needs to learn the same tasks but in different domains. Task identities are not required.

In addition to these major scenarios, there are also other scenarios present in the literature like task-free continual learning (TFCL), online continual learning (OCL), blurred boundary continual learning (BBCL), continual pre-training (CPT), we refer to Wang et al. for a thorough study.

3.2. Multimodal Dataset

The multimodal dataset comprises two components: sensor signals from an actuated finger and non-stationary images of objects captured by a vision camera. The two different modalities are fused into a hybrid setup that incorporates both class incremental as well as domain incremental scenarios as illustrated in Figure 1. In this setup, progression from left to right represents class-incremental training, while progression from top to bottom represents domain-incremental training. Both domains encompass five tasks, with each task involving the learning of two new classes. The first domain focuses on sensor signal data for various objects encountered in each experience and follows a class-incremental learning approach. The second domain deals with visual data of the same objects and employs both domain-incremental and class-incremental learning methods. Further details on data collection for the different modalities are provided in the subsequent sections.

3.2.1. Sensor Signal

To collect the sensor signals for the different objects we utilize a soft pneumatic gripper Hao et al. equipped with four sensors which are affixed together using stretchable nylon thread as illustrated in Figure 10. We have employed the commercially available flex sensors Saggio et al., Mishra et al. to measure the bending of the finger and a force sensitive resistor (FSR) Hollinger and Wanderley to quantify the force applied to the fingertip as shown in Figure 2. The outputs from the flex and force sensors are directed to an Arduino Due board, which in turn is connected to a computer for further processing and analysis. We gather the sensor data for 10 distinct objects, for each object the gripper acquires 50 data points, considering various orientations of the object. During the data collection process, for each data point the gripper holds and releases the object repeatedly at different contact points, with each cycle lasting ~ 39 seconds. Each data point is represented as a 600-dimensional vector, encapsulating the sensor signals recorded during that time interval. The dataset acquisition for every object takes about 37 minutes to complete on a computer equipped with an Intel Core i7 CPU @2.80GHz (GTX 1070 GPU) running Windows 10.

3.2.2. Image Data

The image data consists of the same classes but repeated with three different objects. Each object is repeated 3 times to create a more diversified dataset. Classification can be performed at object level (30 classes) or at category level (10 classes). For each trial, the images are extracted from a 15-second video sequence at a rate of 10 frames per second (FPS). Objects are hand-held by the operator and the camera point-of-view is that of the operator's eyes. The operator extends his arm and smoothly rotates the object in front of the camera. The grabbing hand (left or right) changes throughout the sessions and relevant object occlusions are often produced by the hand itself. This creates a complex non-stationary dataset with variable lighting conditions and

arbitrary amounts of occlusion produced by the operator's hand. The final dataset consists of 13,500 RGB images each of size 128x128 extracted from the video frame. The images are further resized to 32x32 dimension to speed up the training and evaluation process.

3.3. Evaluation Metrics

The performance of the CL algorithm depends on its ability to adapt, retain, and generalize the knowledge over time. We evaluate the incremental accuracy (denoted as a_t) of the model after every task as well as the average accuracy over all the tasks for each domain denoted as A_T . The average accuracy over all the domains is referred to as A_D in the paper. We define the expressions as follows:

$$A_T = \frac{1}{T} \sum_{t=1}^{T} a_t \quad A_D = \frac{1}{D} \sum_{T=1}^{T=D} A_T \quad (1)$$

where T and D refer to the total number of incremental tasks in each domain and the total number of domains.

To evaluate the SSL capabilities of the algorithm we perform two different experiments as proposed in the paper Smith et al., we use the following terminology to describe them: First, *Random Images*, where we have 20% of unlabeled data and 80% labeled data for each class. To collect the unsupervised data we randomly sample 20% (about 240) data from the training dataset for each class, remove the class label, shuffle, and store it in a separate folder. Second, *Unseen Images*, where we sample the images of an unseen object of the same parent class from the training dataset and repeat the above steps. A point to note is that in the first case, the model might have already seen all the objects for each class, however for the second case, the model has never seen the objects present in the unsupervised dataset and thus makes it a more challenging situation. In addition, we also perform an ablation study to show the effectiveness of the intra-layer feature representation as well as SSL on the model's overall accuracy.

4. Methodology

In this section, we discuss the modifications made to the FeCAM algorithm Goswami et al.. Originally, the algorithm models the feature distribution of classes using a multivariate normal distribution, $\mathcal{N}(\mu, \Sigma)$, and uses the Mahalanobis distance to perform classification. While the authors proposed several techniques to enhance and stabilize Mahalanobis-based distance classification, one significant limitation of FeCAM is its requirement to store batches in temporary memory and conduct training only once all data for a particular task is available. This makes it unsuitable for online learning. To address this issue and improve the algorithm's capability for multimodal training, as well as to adapt to the semi-supervised nature of the dataset, we introduce several new features to the exFeCAM algorithm, which are detailed below.

Table 1

Pre-train model architecture for both the domains of the custom multimodal dataset, domain 2 represents the image data and domain 1 signifies the sensor data. The linear layers for both the models are removed once the pre-training is completed. Here, "classes" refers to the total number of output classes during the pre-training phase.

Model type	Layer type	Activation function	Output channel/neurons	Batch Normalization	Other details
Domain 2	Conv2D	Relu	16	Batchnorm2D	kernel:3, stride:1, padding:1
	Conv2D	Relu	32	Batchnorm2D	kernel:3, stride:2, padding:1
	Conv2D	Relu	64	Batchnorm2D	kernel:3, stride:2, padding:1
	Conv2D	Relu	64	Batchnorm2D	kernel:3, stride:3, padding:0
	Conv2D	Relu	128	Batchnorm2D	kernel:2, stride:2, padding:0
	Flatten	-	-	-	-
	Linear	Relu	2000	-	-
	Linear	Relu	1000	-	-
	Linear	Relu	classes	-	-
Domain 1	Conv1D	Leakyrelu (0.01)	512	Batchnorm1D	kernel:3, stride:1, padding:1
	Conv1D	Leakyrelu (0.01)	256	Batchnorm1D	kernel:3, stride:2, padding:1
	Conv1D	Leakyrelu (0.01)	128	Batchnorm1D	kernel:3, stride:2, padding:1
	Flatten	-	-	-	-
	Linear	Relu	256	-	-
	Linear	-	classes	-	-

4.1. Online Batchwise Training

Online training involves training a model incrementally in a batch-wise manner rather than on the entire dataset for a particular task at once. In this approach, each batch of data is passed through a feature extractor to obtain feature maps, which are then used to calculate the prototypes (mean and co-variance matrix) for each class in that batch. A dictionary is initialized with class labels as keys and their corresponding prototypes as values. There are two possible scenarios when updating this dictionary:

1. If a class is encountered for the first time, a new entry is added with the class label as the key and the prototypes as the value.
2. If the class has been seen before, the existing prototypes for that class are retrieved and updated by averaging the previous prototypes with the new ones from the current batch.

This method avoids the need to store incoming data for each task, which is critical for continual learning (CL) objectives and is especially suitable for autonomous agents with limited cache memory. Learning prototypes in a batch-wise manner addresses the challenge of not having access to previous data points, making it a more practical solution for real-time applications.

4.2. Intra Layer Feature Representation

Intra-layer feature representation (ILFR) leverages the power of intermediate layers that encodes the low and mid-level feature information present in the data extracted using a pre-trained model. Instead of relying solely on the final output layer of the feature extractor, the presence of multiple activation maps generalizes the learned knowledge and further improves the performance of the algorithm. We argue

that enriching the last layer representations with hierarchical intra-layer features increases robustness to domain shifts and thus improves generalizability to downstream continual tasks. These extracted features can be the class embeddings of a transformer encoder Vaswani et al. or flattened feature maps of a ResNet encoder He et al..

There are two intuitive ways to promote intra-layer feature representations into the model: averaging the representations from the last "k" layers of the network or concatenating the representations from the last k layers. The first approach requires the output dimensions of all layers to be identical to facilitate summation. In our use case, we opt for concatenation, as the outputs from different layers have varying dimensions. Concatenation also preserves the rich, multi-scale features, unlike summation, which can result in information loss due to the merging of complementary features captured by different layers, potentially reducing the richness of the learned representations.

For the multimodal experiment, we pre-train the domain 1 feature extractor on gripper data of objects not present in the training dataset, while the domain 2 feature extractor is trained on the Core50 dataset. More details about the pre-trained model architecture are provided in Table 1. For the Core50 experiment, we use the ResNet18 architecture as the feature extractor, pre-trained on the ImageNet1k dataset Russakovsky et al..

4.3. Semi-Supervised Learning

Semi-supervised learning (SSL) denotes the capability of an algorithm to learn from supervised data and then improve the performance of the model by training it on the unsupervised part. It is very useful in a situation where we have limited supervised data but we can collect huge amounts of unsupervised data from the environment. This is

Algorithm 1 exFeCAM Algorithm

Input: Data stream $(D_0^0, D_0^1, \dots, D_1^0, D_1^1, \dots, D_n^{0:t})$, where " t " refers to the number of tasks, " n " refers to the number of domains.

Models: Feature extractor $f_e(x; \theta_e)$, exFeCAM model $\phi(x; \mu, \Sigma)$

Variables: k : number of layers of feature extractor, t : total tasks, n : number of domains, T : total classes; b : batch size; l, j : iterative variables

$(x_i, y_i) \in D_{train}^{Supervised}$, $(x'_i) \in D_{train}^{Unsupervised}$, $(x''_i, y''_i) \in D_{test}$

$\mu, \Sigma = \{\}$

▷ Initialize μ, Σ

Training Phase

for $E_i \in [E_0, E_1, \dots, E_t]$ **do**

▷ Different tasks/experiences

Temporary Buffer (ϵ) $\leftarrow \{\}$

▷ Temporary memory buffer for feature matching

for $y_i \in [y_0, y_1, \dots, y_T]$ **do**

▷ Classes in each task

for $j \leftarrow b$ **do**

$\psi_{ij} \leftarrow [f_e(x_i)_{k-(l-1)}, f_e(x_i)_{k-(l-2)}, \dots, f_e(x_i)_k]$

▷ Concatenate intra layer feature

$\mu[i] \leftarrow \frac{1}{b} \sum \psi_{ij}$

▷ Mean matrix

$\Sigma[i] \leftarrow \text{Covariance}(\psi_{ij})$

▷ Covariance matrix

$\Sigma[i]_S \leftarrow \text{Shrinkage}(\Sigma[i])$

$\Sigma[i]_N \leftarrow \text{Normalization}(\Sigma[i]_S)$

if ϵ is not empty **then**

similarity $\leftarrow \text{cosine similarity}(\text{features} \in \epsilon, x'_i)$

▷ Compute cosine similarity

if similarity \geq threshold **then**

Update $\mu[i], \Sigma[i]_N$

▷ Update the mean and cov matrix for each class

end if

end if

end for

end for

end for

Test Phase

for $x''_i \in D_{test}$ **do**

$\phi(f_e(x''_i); \mu, \Sigma) \leftarrow (f_e(x) - \mu_i)^T (\Sigma_i)^{-1} (f_e(x) - \mu_i)$

▷ Calculate the Mahalanobis distance

$y_{pred} \leftarrow \text{argmin} \phi(f_e(x''_i); \mu, \Sigma) \forall y_i = 0, 1, \dots, T$

▷ Assign the class with minimum Mahalanobis distance

end for

an active area of research given that large, labeled datasets are expensive, but most applications have access to plentiful, cheap unlabeled data. In this paper, we use the concept of pseudo-labeling to organize the unsupervised data and provide them with dummy labels for further training. To perform pseudo labeling we randomly store the feature maps of each class for every task in a temporary memory buffer and then perform cosine similarity between the reference feature maps and the feature maps generated from the complete unsupervised dataset as defined in equation 2,

$$\text{similarity} = \frac{x_1 \cdot x_2}{\|x_1\|_2 \|x_2\|_2} \quad (2)$$

where x_1 and x_2 refers to the reference feature map present in the temporary memory and the feature maps from the unsupervised dataset, $\|\cdot\|_2$ refers to the l2 norm of the two tensors. If the value of the cosine similarity is greater than a certain threshold, we then train the exFeCAM algorithm on the respective feature maps and its associated pseudo labels. These pseudo-labels are derived from the class labels used for feature matching. The prototype values for that class are subsequently updated using the averaging rule described in the previous section. To determine the threshold value,

we employ the Optuna framework Akiba et al., which uses bayesian optimization to explore the hyperparameter space efficiently.

4.4. Multimodal Training

We extend the class-incremental continual learning to a more realistic semi-supervised continual learning (SSCL) setting, where data distributions reflect existing object class correlations between, and among, the labeled and unlabeled data distributions. For our experiment we use 70% labeled data and 30% unlabeled data for the two protocols (random and unseen) discussed above. At task n , we denote batches of labeled data as $X_n = (x_b, y_b) : b_i \in (1, \dots, b) | y_b \in \tau_n$ and batches of unlabeled data as $X'_n = (x'_b) : b_i \in (1, \dots, b)$, where b refers to the batch size. The goal in task n is to learn a model which predicts object class labels for any query input over all classes seen in the current and previous tasks $(\tau_0 \cup \tau_1 \cup \dots \cup \tau_n)$. During each training step the model receives different classes incrementally over all the experiences for each domain as shown in Figure 1. The two domains contain data from different modalities specifically domain 1 contains the sensor data whereas domain 2 contains the vision data. The data for each task goes through a feature extractor to

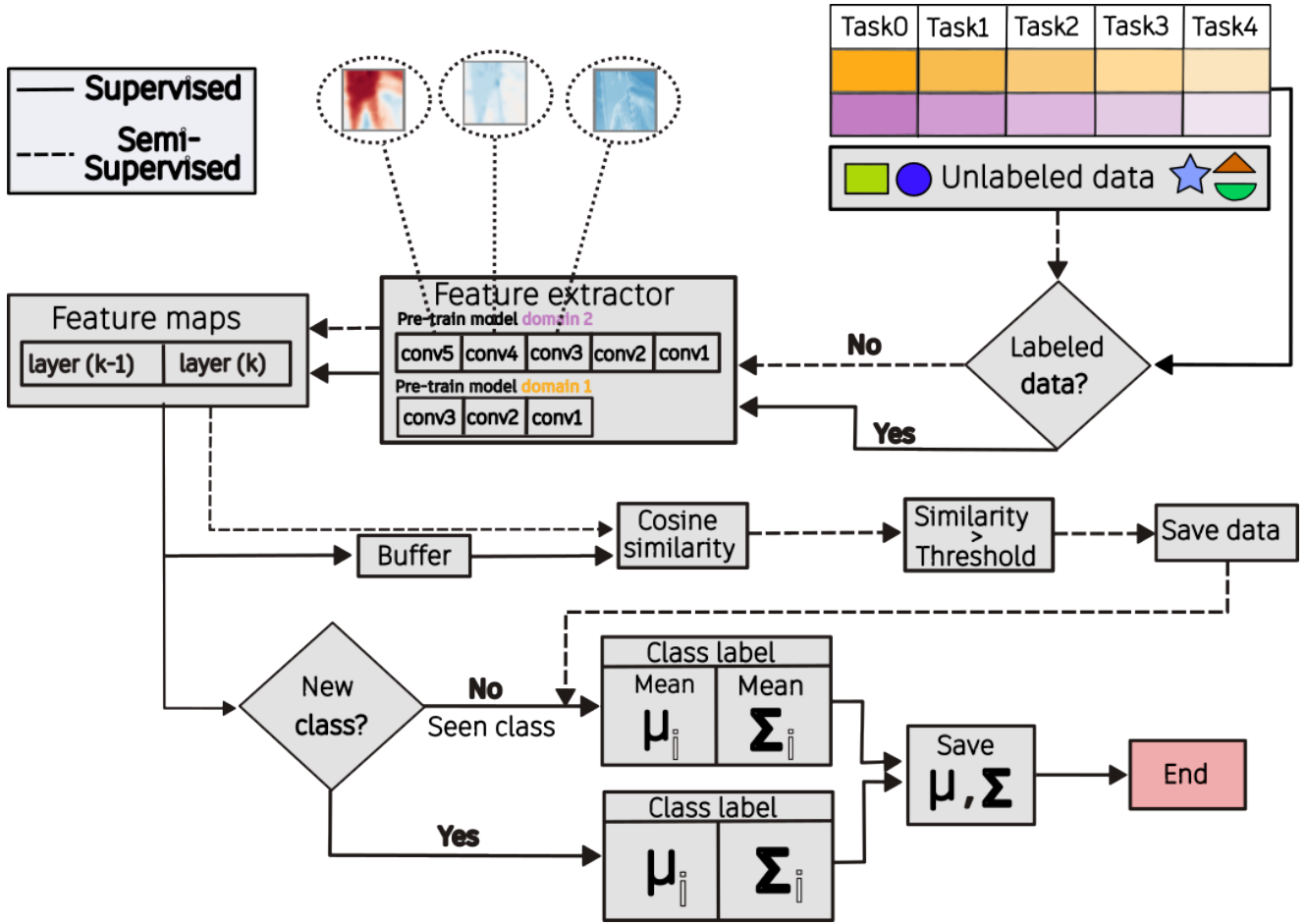


Figure 3: Modified FeCAM algorithm with intra layer feature representation, online batchwise learning, and semi-supervised learning capabilities for multimodal training. During training on multiple domains, the algorithm stores the mean and covariance matrices of the classes in a dictionary. In the testing phase, the algorithm uses these stored prototypes and employs the Mahalanobis distance to determine the prediction class. Supervised training is depicted with solid black lines, while unsupervised training is illustrated with dashed black lines.

derive the feature maps from the different layers of the network. The feature maps for both domains are standardized to a fixed dimension of 384 and normalized to fall within the 0-1 range before being fed into the subsequent stages of the algorithm. These feature maps are then used to incrementally train the exFecam algorithm. During training for each task in the second domain, a small subset of the feature maps of the object is stored in a temporary memory buffer to facilitate pseudo-labeling for semi-supervised learning, as previously discussed.

The feature maps are used to compute the mean and covariance matrix for each batch during training. The model performs covariance matrix approximation, shrinkage, and normalization to stabilize the training process *Goswami et al.*. During the test phase, the extracted feature maps from the test dataset are used to calculate the Mahalanobis distance for all seen classes, and the class with the minimum distance value is selected as the output class. More details about the implementation of the algorithm is provided in the pseudo code. Additionally, we also perform a real-time test

for object classification based on the multimodal data using the ROS framework as discussed in section 6 of the paper.

We further analyzed the intra-layer feature representation for both the custom dataset and the Core50 dataset by comparing the accuracy improvement of the exFeCAM algorithm when incorporating knowledge from the last and penultimate layers of pre-trained feature extractors. The Core50 dataset showed a significantly greater improvement in accuracy compared to the custom dataset. The difference is attributed to the more diverse information contained in the image data of the Core50 dataset.

5. Results

To assess the performance of our algorithm and the effectiveness of the proposed modifications, we evaluate the exFeCAM algorithm on a custom multimodal dataset and the standard Core50 dataset used in the literature. The Core50 dataset was chosen for its non-iid nature and its compatibility for self-supervised learning. We do not explicitly

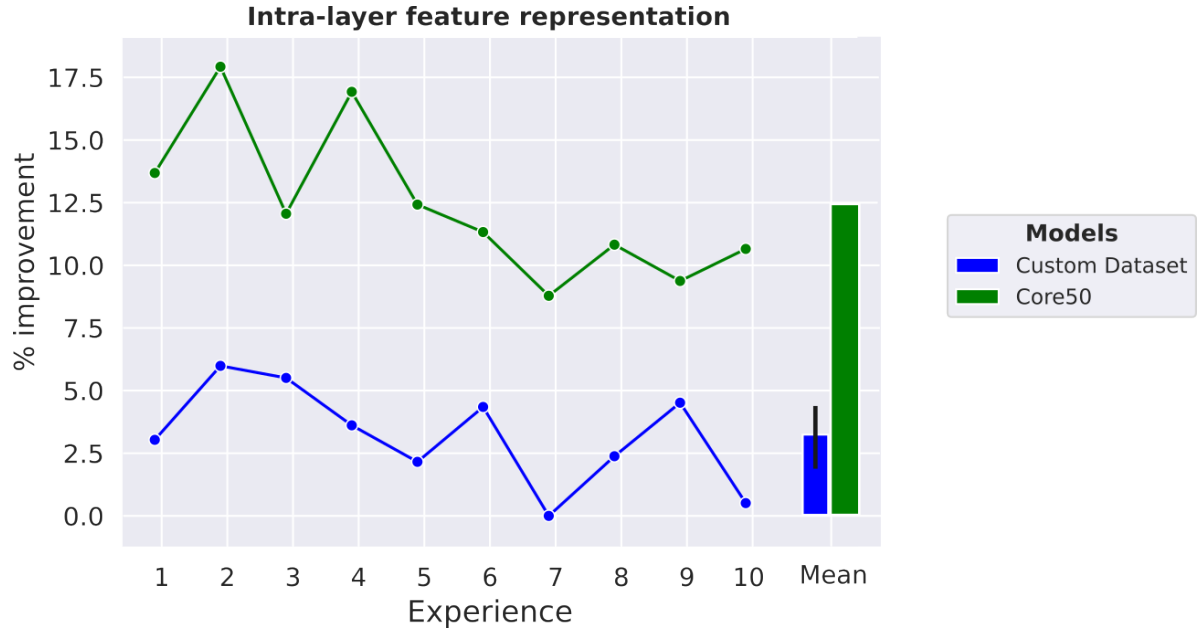


Figure 4: Intra layer feature representation for the custom dataset and the Core50 dataset, we compare the improvement in the accuracy of the FeCAM algorithm on addition of knowledge from the last as well the penultimate layers of the pre-trained feature extractors. The improvement in case of Core50 dataset is considerably more than the custom dataset due to the presence of more diverse information in case of image data.

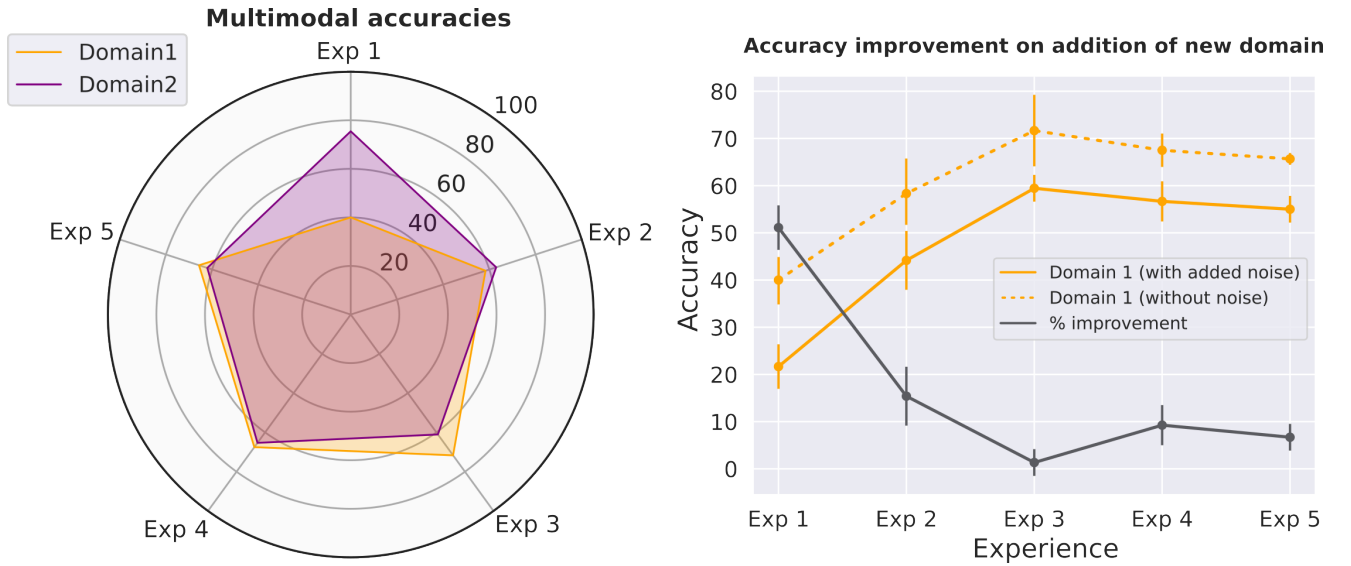


Figure 5: On the left: radar plot shows the accuracy of the two domains after incremental training on different tasks. The FeCAM algorithm learns the first domain in a class-incremental approach, while it learns the second domain in a combined domain-incremental and class-incremental manner. On the right: the plot shows domain 1 accuracy (in orange) with random gaussian noise added to it, the solid line in grey shows the percentage improvement in the overall accuracy of the experiences after addition of the second domain. The black lines show the error bars for the two cases.

compare our algorithm with other state-of-the-art (SOTA) benchmarks because the focus of this paper is not to establish a new level of accuracy for object classification, but rather to demonstrate the effectiveness of CL in a real world multi-modal training setting. Nevertheless, our results are based on improvements to the original FeCAM algorithm, indirectly providing a comparison. All experiments are repeated three

times, and we plot the mean and standard deviation of the respective metrics.

Figure 4 demonstrates the improvements in our algorithm's prediction accuracy with the inclusion of intra-layer feature representation. For the custom dataset (plotted in green), the first five experiences illustrate the percentage

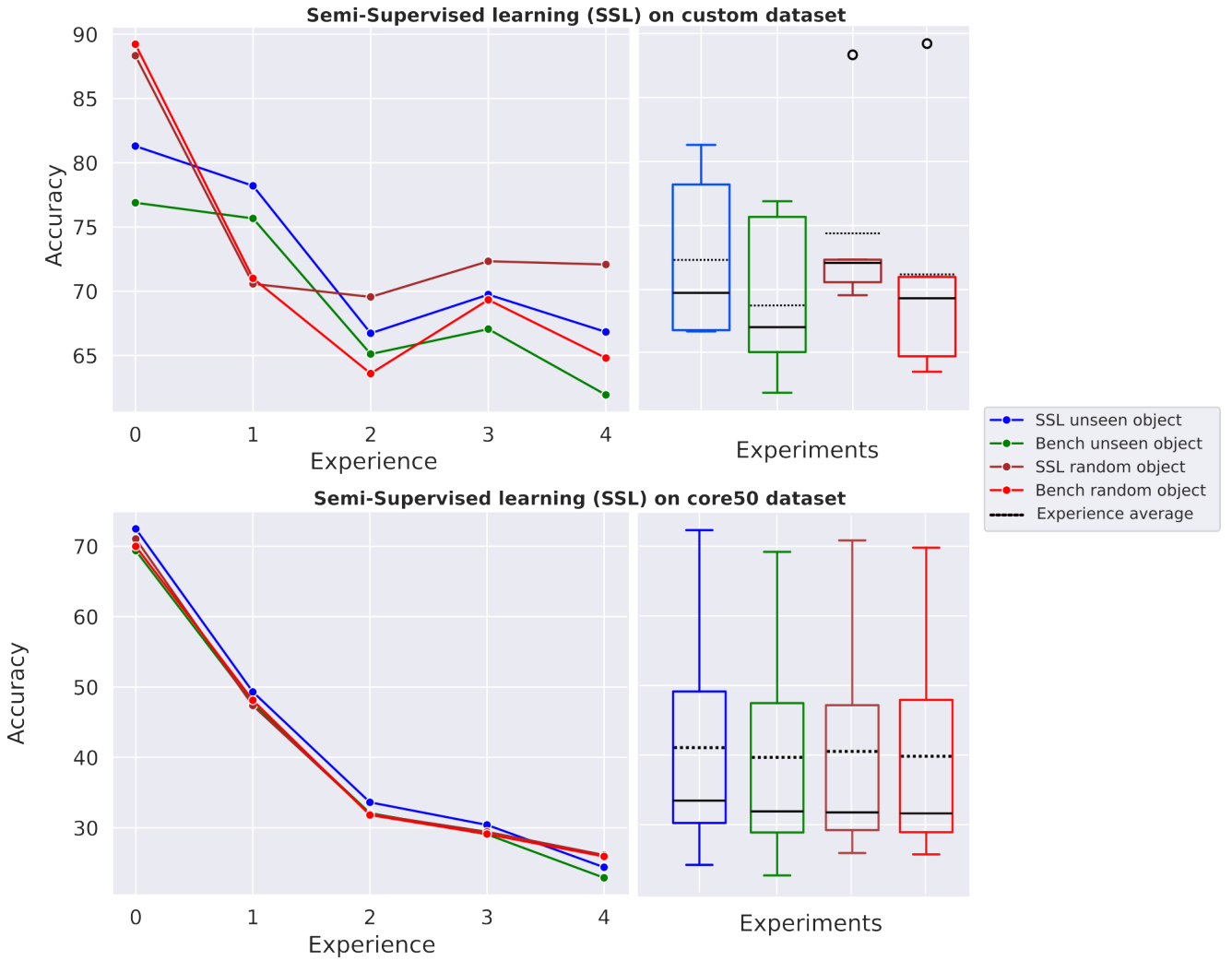


Figure 6: Accuracy of the FeCAM algorithm on SSL tasks, the blue and green plot shows the SSL condition for unseen object from the same parent class, with blue indicating SSL enabled and green indicating SSL disabled case. The maroon and red plots represent the SSL condition for randomly selected images of the object, with maroon indicating SSL enabled and red indicating SSL disabled case. Top plot shows the accuracy for the custom multimodal dataset and the bottom plot shows the accuracy for the Core50 dataset. The black dotted lines denotes the average accuracy over all the experiences for different SSL cases.

improvement in domain 2 data, while the next five experiences indicate the accuracy improvement in domain 1. Each experience comprises two different classes for both the domains. The improvement magnitude for domain 2 is slightly greater than domain 1. The overall improvement for the custom dataset experiment is approximately $3.21 \pm 1.43 \%$, with domain 2 contributing about 1.71% more than domain 1. This can be attributed to the presence of image data in domain 2, which offers more diverse information across different network layers compared to sensor signal data. This trend is further validated by the core50 experiment (shown in blue), where all 10 experiences involve images, each containing five random classes. In this case, the overall improvement is around $12.39 \pm 0.0 \%$ compared to the original FeCAM algorithm without intra-layer feature representation.

The CL capability of the exFeCAM algorithm is depicted in Figure 5 (left). The spider plot displays both class incremental and domain incremental accuracy for the two modalities. The class incremental accuracy for the sensor data is represented in orange, while the violet plot corresponds to the combined domain incremental and class incremental scenario for the image data. The results demonstrate that the model can learn new modalities while preserving information from previous ones. The per task accuracy for each domain is clearly visible in the spider plot, and the mean accuracy after completion of all the tasks for domain 1 is $60.63 \pm 6.15\%$ whereas for domain 2 is $65.36 \pm 0.0 \%$. One of the reasons for higher variability in domain 1 can be due to the presence of relatively small sample sizes for training and testing. However, this experiment does not take into consideration the SSL capability of the algorithm and is trained on the complete data in a supervised manner.

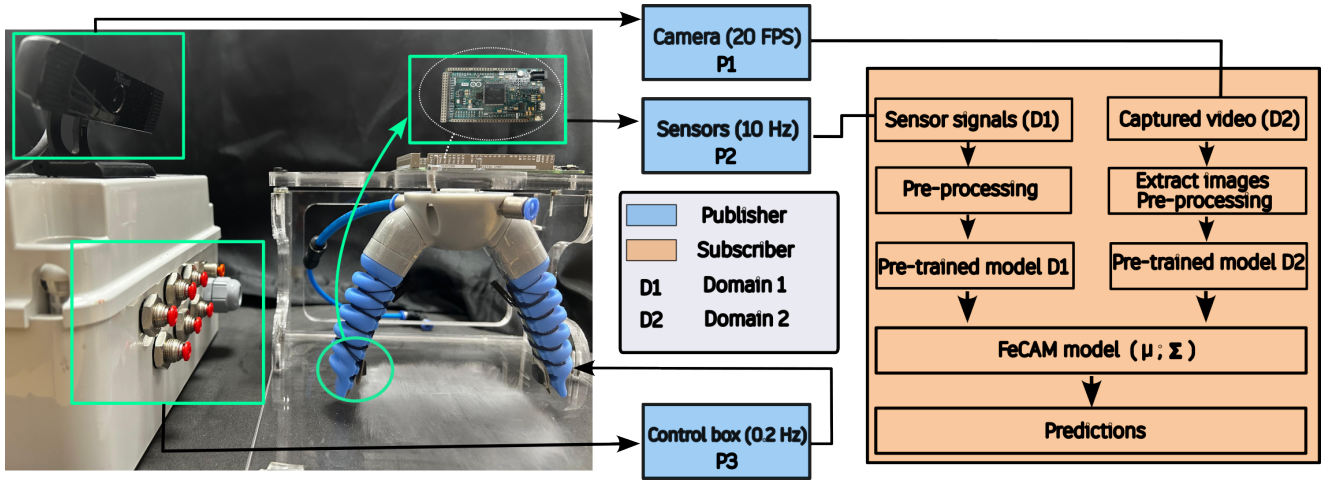


Figure 7: The real-time multimodal experiment using ROS involves three publishers and one subscriber node. The publishers (P1, P2, P3) are depicted in blue, while the subscriber is shown in yellow. P1 operates at a frequency of 20 Hz, P2 operates at 10 Hz, and P3 operates at 0.2 Hz. The output from P3 is used to actuate a soft finger equipped with sensors. The outputs from P1 and P2 are fed to the subscriber, where they undergo pre-processing, feature extraction using a pre-trained network, and finally to the FeCAM algorithm to make the predictions using the saved mean and co-variance matrices.

Figure 5 (right) demonstrates the advantage of training on a new domain when the information from the first domain (sensors signal) is noisy. To simulate this scenario, gaussian noise was added to the sensor signal data. The solid orange line indicates the accuracy across different experiences for domain 1 with noisy sensor data, while the dashed orange line shows the original accuracy without noise. The solid grey line represents the percentage improvement in accuracy across different experiences when the second domain is added to compensate for the accuracy loss due to the noisy data in domain 1.

To demonstrate the SSL capabilities, we conducted two distinct types of experiments in the SSL setting, as discussed in Section 3.3. Figure 4 (top) illustrates the accuracy of the custom dataset within the SSL framework. It is important to note that the SSL technique is applied exclusively to the image data due to the presence of multiple objects for each class. The blue plot depicts the accuracy of the exFeCAM algorithm for the *unseen object* scenario with SSL enabled, while the green plot shows the accuracy for the same scenario but with SSL disabled. The plots clearly demonstrate that incorporating information about new unseen objects enhances the accuracy over each experience. Similarly, for the *random object* scenario, the model's accuracy with SSL, shown in brown, surpasses that of the benchmark case without SSL capabilities, indicated in red. The box plots provide detailed information about the highest and lowest accuracy, the median value (represented by a solid black line), the mean value (represented by a dotted black line), and the Q1 and Q3 quartiles, which encompass approximately 25 % to 75 % of the overall accuracy.

Figure 4 (bottom) presents similar information for the Core50 dataset, where we employed the same experimental protocols. The key difference lies in the pre-trained model

and the pre-training dataset used in this experiment. However, the improvement in accuracy for the Core50 dataset is minimal compared to the custom dataset. This could be attributed to the significant variations in the objects within each class, making the simple cosine similarity method less effective in this context. A more complex SSL method might be more beneficial for this scenario, which we plan to explore in future experiments.

6. Real-Time Evaluation With ROS

Robot Operating System (ROS) is a comprehensive framework that comprises a suite of tools, libraries, and protocols aimed at facilitating the development of various robotic systems. The system manages the creation and control of communication between a robot's peripheral modules, such as sensors, cameras, and actuators, thereby enabling the seamless integration of these components with parallelization capabilities.

6.1. ROS Setup

ROS is primarily designed to function optimally on Ubuntu, while only partially compatible with other operating systems, such as Windows and Mac. For our case we use ROS on Ubuntu 20.04 on a Intel Core i7 7th gen CPU @ 2.80 GHz equipped with Nvidia GTX 1080 GPU. We use the Noetic Ninjemys distribution of ROS 1 Koubaa et al. in our experiment. A detailed explanation about the workflow of the project is provided in the flowchart in Figure 7. The first publisher (P1) publishes the sensor signals coming from the four sensors attached to the soft finger, the second publisher (P2) publishes the video coming from the camera and the third publisher (P3) publishes the command pressure to the control box which in turn actuates the finger. The control frequency of P1 and P2 are 10hz and 20hz, whereas the

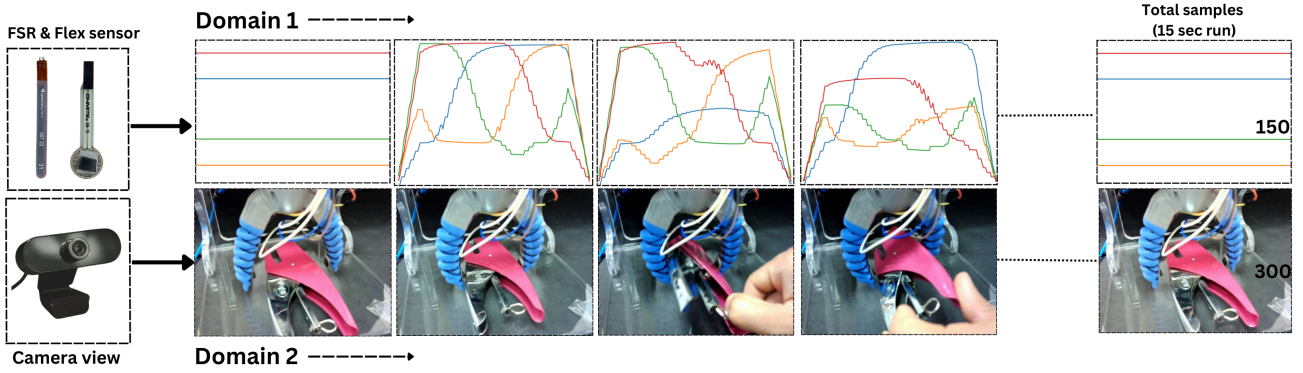


Figure 8: Real-time images of the object from the camera's perspective, along with the sensor data from four sensors attached to the soft finger, upon its actuation. These images and sensor readings are directly fed into the FeCAM model after resizing them to the desired dimension. For a single 15-second run, there are a total of 150 sensor signals and 300 images, representing the number of raw data points and corresponding images of the object.

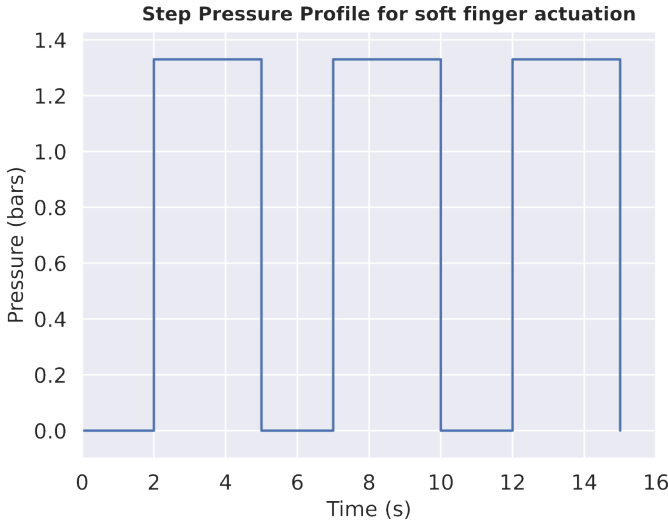


Figure 9: Square wave sent to the control box to actuate the soft pneumatic finger. We pressurise the finger for 3 seconds with a maximum pressure of 1.3 bars and then depressurise it for 2 seconds, the cycle is repeated "N" times till we reach the 15 seconds threshold for each run.

actuation frequency of P3 is 0.2hz. We further observed that actuating the finger at a more higher frequency constrained it from properly holding the object and thus effected the quality of the generated data from the sensors. The data from P1 and P2 goes to the subscriber which then pre-process the data, extracts the frames from the video in case of P2 and sends it to the respective feature extractors. The output of the feature extractor is a 384-dimensional feature map (in case the intra-layer feature representation is turned on) which goes as an input to the exFecam model for further processing.

6.2. Real-Time Experiment

To assess the performance of our algorithm, we conduct a quasi real-time experiment using a soft pneumatic gripper

equipped with two flex sensors and two force sensors. During the evaluation phase, data from the sensors and the camera are collected in real-time for approximately 15 seconds. These data are treated as two distinct domains and are sent through the pipeline in parallel for further processing and subsequently to the exFecam model for predictions. To generate the predictions we utilize the stored mean and the covariance matrix from a prior offline incremental experiment conducted for the two domains. Impressively, the mean and covariance matrix occupy only 22.5 MB of memory, making it quite efficient compared to other continual learning strategies

However, since the model was initially trained on images of the objects in a different frame of reference, where the operator extends his arm and smoothly rotates the object in front of the camera. In contrast, during the real-time experiment, the objects are positioned near the soft finger, and a camera captures images from a top-down view. This difference sometimes leads to incorrect predictions by the model. To address this issue, for some objects, we occasionally need to refine the model's knowledge by conducting a brief training session (lasting around 82 seconds) specifically for that object. Figure 8 shows a snapshot of the real-time data collection from both the sensors and the camera's perspective. The image shows the progression of the sensor signal and the camera image upon actuating the finger. For each cycle the sensors collect 150 raw values, which are transformed into a single 600-dimensional vector, whereas the camera collects around 300 images of the object from various orientations within the 15-seconds interval.

As discussed above one of the major advantages of this domain incremental training is for autonomous agents in situations where the field of view of one of the sensors gets restricted due to the presence of some obstacle from the environment, in that case the presence of other sensor can compensate for the missing knowledge.

6.3. Real World Application

A real world application for such a technique can be in companion robots Broadbent et al., where the robot learns new tasks incrementally by interacting with its environment and recognizing different objects using information from multiple sensors available to it. The use of multiple sensors is particularly advantageous in scenarios where a single sensor cannot provide complete information about an object. For instance, a vision camera might struggle to differentiate between two objects with similar structures but with different textures or materials, with one being much softer than the other. In such cases, information from a tactile sensor can be extremely beneficial. Our proposed framework simplifies the addition of new sensors by treating each as a new domain, eliminating the need to retrain the entire algorithm from scratch each time. All the sensors and the algorithm can be synchronized using a mobile version of ROS for embedded systems Min et al., providing a comprehensive solution.

7. Conclusion and Discussion

In this paper, we present a novel continual learning method that combines the informations from different sensors in a domain incremental fashion while also learning new classes or objects in a class incremental manner. We enhanced the original FeCAM algorithm by incorporating online batch-wise training, intra-layer feature representation, and SSL capabilities thereby making the algorithm suitable for our scenario. The exFeCAM algorithm employs cosine similarity based feature matching to perform pseudo labeling when encountering unlabeled data. We validated the algorithm on two different modalities of data namely sensor signal based data and image based data, and demonstrated the ability of the algorithm to learn the two modalities incrementally. We also conducted an ablation study to show the contribution of different parts of the algorithm. Additionally, we performed a real-time experiment on a soft pneumatic gripper equipped with four sensors and an external camera system, all synchronised using the ROS framework. As part of our future work, we aim to enhance the exFeCAM algorithm further by adding forward and backward knowledge capabilities, either through interactions between class prototypes or by training a simple multilayer perceptron (MLP) network to learn these interactions. Moreover, currently we need to manually select the prediction domain modality in the presence of noise; in the future, we aim to enable the algorithm to automatically determine this by calculating the confidence of each prediction from the network.

CRedit authorship contribution statement

Nilay Kushawaha: Writing - original draft, Methodology, Investigation, Experimentation, Formal Analysis, Conceptualization. **Egidio Falotico:** Supervision, Funding acquisition, Project administration.

Declaration of competing interest

The authors declare that they have no known competing financial interests or personal relationships that could have appeared to influence the work reported in this paper.

Data availability

Data will be made available on request. The code is available on the github repo : <https://github.com/nilay121/Multimodal-Fusion-using-CL>

Acknowledgment

We acknowledge the contribution from the Italian National Recovery and Resilience Plan (NRRP), M4C2, funded by the European Union–NextGenerationEU (Project IR0000011, CUP B51E22000150006, "EBRAINS-Italy")

References

- [1] M. Ahmad, S. Shabbir, S. K. Roy, D. Hong, X. Wu, J. Yao, A. M. Khan, M. Mazzara, S. Distefano, J. Chanussot, Hyperspectral image classification—traditional to deep models: A survey for future prospects, *IEEE journal of selected topics in applied earth observations and remote sensing* 15 (2021) 968–999.
- [2] Z. Zou, K. Chen, Z. Shi, Y. Guo, J. Ye, Object detection in 20 years: A survey, *Proceedings of the IEEE* 111 (2023) 257–276.
- [3] D. W. Otter, J. R. Medina, J. K. Kalita, A survey of the usages of deep learning for natural language processing, *IEEE transactions on neural networks and learning systems* 32 (2020) 604–624.
- [4] L. Wang, X. Zhang, H. Su, J. Zhu, A comprehensive survey of continual learning: theory, method and application, *IEEE Transactions on Pattern Analysis and Machine Intelligence* (2024).
- [5] T. Lesort, V. Lomonaco, A. Stoian, D. Maltoni, D. Filliat, N. Díaz-Rodríguez, Continual learning for robotics: Definition, framework, learning strategies, opportunities and challenges, *Information fusion* 58 (2020) 52–68.
- [6] J. E. Van Engelen, H. H. Hoos, A survey on semi-supervised learning, *Machine learning* 109 (2020) 373–440.
- [7] D. Goswami, Y. Liu, B. Twardowski, J. van de Weijer, Fecam: Exploiting the heterogeneity of class distributions in exemplar-free continual learning, *Advances in Neural Information Processing Systems* 36 (2024).
- [8] V. Lomonaco, D. Maltoni, Core50: a new dataset and benchmark for continuous object recognition, in: *Conference on robot learning*, PMLR, 2017, pp. 17–26.
- [9] A. Koubaa, et al., *Robot Operating System (ROS)*, volume 1, Springer, 2017.
- [10] A. A. Rusu, N. C. Rabinowitz, G. Desjardins, H. Soyer, J. Kirkpatrick, K. Kavukcuoglu, R. Pascanu, R. Hadsell, Progressive neural networks, *arXiv preprint arXiv:1606.04671* (2016).
- [11] C. Fernando, D. Banarse, C. Blundell, Y. Zwols, D. Ha, A. A. Rusu, A. Pritzel, D. Wierstra, Pathnet: Evolution channels gradient descent in super neural networks, *arXiv preprint arXiv:1701.08734* (2017).
- [12] J. Rajasegaran, M. Hayat, S. H. Khan, F. S. Khan, L. Shao, Random path selection for continual learning, *Advances in neural information processing systems* 32 (2019).
- [13] R. Aljundi, P. Chakravarty, T. Tuytelaars, Expert gate: Lifelong learning with a network of experts, in: *Proceedings of the IEEE conference on computer vision and pattern recognition*, 2017, pp. 3366–3375.
- [14] A. Mallya, D. Davis, S. Lazebnik, Piggyback: Adapting a single network to multiple tasks by learning to mask weights, in: *Proceedings of the European conference on computer vision (ECCV)*, 2018, pp. 67–82.

- [15] J. Serra, D. Suris, M. Miron, A. Karatzoglou, Overcoming catastrophic forgetting with hard attention to the task, in: International conference on machine learning, PMLR, 2018, pp. 4548–4557.
- [16] A. Mallya, S. Lazebnik, Packnet: Adding multiple tasks to a single network by iterative pruning, in: Proceedings of the IEEE conference on Computer Vision and Pattern Recognition, 2018, pp. 7765–7773.
- [17] H. Ahn, S. Cha, D. Lee, T. Moon, Uncertainty-based continual learning with adaptive regularization, *Advances in neural information processing systems* 32 (2019).
- [18] J. Kirkpatrick, R. Pascanu, N. Rabinowitz, J. Veness, G. Desjardins, A. A. Rusu, K. Milan, J. Quan, T. Ramalho, A. Grabska-Barwinska, et al., Overcoming catastrophic forgetting in neural networks, *Proceedings of the national academy of sciences* 114 (2017) 3521–3526.
- [19] F. Zenke, B. Poole, S. Ganguli, Continual learning through synaptic intelligence, in: International conference on machine learning, PMLR, 2017, pp. 3987–3995.
- [20] A. Chaudhry, P. K. Dokania, T. Ajanthan, P. H. Torr, Riemannian walk for incremental learning: Understanding forgetting and intransigence, in: Proceedings of the European conference on computer vision (ECCV), 2018, pp. 532–547.
- [21] R. Aljundi, F. Babiloni, M. Elhoseiny, M. Rohrbach, T. Tuytelaars, Memory aware synapses: Learning what (not) to forget, in: Proceedings of the European conference on computer vision (ECCV), 2018, pp. 139–154.
- [22] G. Hinton, O. Vinyals, J. Dean, Distilling the knowledge in a neural network, *arXiv preprint arXiv:1503.02531* (2015).
- [23] Z. Li, D. Hoiem, Learning without forgetting, *IEEE transactions on pattern analysis and machine intelligence* 40 (2017) 2935–2947.
- [24] S.-A. Rebuffi, A. Kolesnikov, G. Sperl, C. H. Lampert, icarl: Incremental classifier and representation learning, in: Proceedings of the IEEE conference on Computer Vision and Pattern Recognition, 2017, pp. 2001–2010.
- [25] P. Dhar, R. V. Singh, K.-C. Peng, Z. Wu, R. Chellappa, Learning without memorizing, in: Proceedings of the IEEE/CVF conference on computer vision and pattern recognition, 2019, pp. 5138–5146.
- [26] K. Lee, K. Lee, J. Shin, H. Lee, Overcoming catastrophic forgetting with unlabeled data in the wild, in: Proceedings of the IEEE/CVF International Conference on Computer Vision, 2019, pp. 312–321.
- [27] D. Lopez-Paz, M. Ranzato, Gradient episodic memory for continual learning, *Advances in neural information processing systems* 30 (2017).
- [28] J. Bang, H. Kim, Y. Yoo, J.-W. Ha, J. Choi, Rainbow memory: Continual learning with a memory of diverse samples, in: Proceedings of the IEEE/CVF conference on computer vision and pattern recognition, 2021, pp. 8218–8227.
- [29] L. Kumari, S. Wang, T. Zhou, J. A. Bilmes, Retrospective adversarial replay for continual learning, *Advances in neural information processing systems* 35 (2022) 28530–28544.
- [30] S. Ebrahimi, S. Petryk, A. Gokul, W. Gan, J. E. Gonzalez, M. Rohrbach, T. Darrell, Remembering for the right reasons: Explanations reduce catastrophic forgetting, *Applied AI letters* 2 (2021) e44.
- [31] G. Saha, K. Roy, Saliency guided experience packing for replay in continual learning, in: Proceedings of the IEEE/CVF Winter Conference on Applications of Computer Vision, 2023, pp. 5273–5283.
- [32] H. Shin, J. K. Lee, J. Kim, J. Kim, Continual learning with deep generative replay, *Advances in neural information processing systems* 30 (2017).
- [33] C. Wu, L. Herranz, X. Liu, J. Van De Weijer, B. Raducanu, et al., Memory replay gans: Learning to generate new categories without forgetting, *Advances in neural information processing systems* 31 (2018).
- [34] A. Ayub, A. R. Wagner, Eec: Learning to encode and regenerate images for continual learning, *arXiv preprint arXiv:2101.04904* (2021).
- [35] B. Pflüß, A. Gepperth, Overcoming catastrophic forgetting with gaussian mixture replay, in: 2021 International Joint Conference on Neural Networks (IJCNN), IEEE, 2021, pp. 1–9.
- [36] Z. Wang, L. Liu, Y. Duan, D. Tao, Continual learning through retrieval and imagination, in: Proceedings of the AAAI Conference on Artificial Intelligence, volume 36, 2022, pp. 8594–8602.
- [37] G. M. Van de Ven, H. T. Siegelmann, A. S. Tolia, Brain-inspired replay for continual learning with artificial neural networks, *Nature communications* 11 (2020) 4069.
- [38] X. Liu, C. Wu, M. Menta, L. Herranz, B. Raducanu, A. D. Bagdanov, S. Jui, J. v. de Weijer, Generative feature replay for class-incremental learning, in: Proceedings of the IEEE/CVF Conference on Computer Vision and Pattern Recognition Workshops, 2020, pp. 226–227.
- [39] F. Ye, A. G. Bors, Learning latent representations across multiple data domains using lifelong vaegan, in: Computer Vision–ECCV 2020: 16th European Conference, Glasgow, UK, August 23–28, 2020, Proceedings, Part XX 16, Springer, 2020, pp. 777–795.
- [40] N. Kushawaha, L. Fruzzetti, E. Donato, E. Falotico, Synapnet: A complementary learning system inspired algorithm with real-time application in multimodal perception, *IEEE Transactions on Neural Networks and Learning Systems* (2024).
- [41] Q. Pham, C. Liu, S. Hoi, Dualnet: Continual learning, fast and slow, *Advances in Neural Information Processing Systems* 34 (2021) 16131–16144.
- [42] G. Petit, A. Popescu, H. Schindler, D. Picard, B. Delezoide, Petril: Feature translation for exemplar-free class-incremental learning, in: Proceedings of the IEEE/CVF winter conference on applications of computer vision, 2023, pp. 3911–3920.
- [43] J. Smith, Y.-C. Hsu, J. Balloch, Y. Shen, H. Jin, Z. Kira, Always be dreaming: A new approach for data-free class-incremental learning, in: Proceedings of the IEEE/CVF international conference on computer vision, 2021, pp. 9374–9384.
- [44] T. L. Hayes, K. Kafle, R. Shrestha, M. Acharya, C. Kanan, Remind your neural network to prevent catastrophic forgetting, in: European conference on computer vision, Springer, 2020, pp. 466–483.
- [45] M. Yan, S. C. Hui, N. Li, Dml-pl: Deep metric learning based pseudo-labeling framework for class imbalanced semi-supervised learning, *Information Sciences* 626 (2023) 641–657.
- [46] C. B. Mawuli, J. Kumar, E. Nanor, S. Fu, L. Pan, Q. Yang, W. Zhang, J. Shao, Semi-supervised federated learning on evolving data streams, *Information Sciences* 643 (2023) 119235.
- [47] A. Rasmus, M. Berglund, M. Honkala, H. Valpola, T. Raiko, Semi-supervised learning with ladder networks, *Advances in neural information processing systems* 28 (2015).
- [48] D. P. Kingma, S. Mohamed, D. Jimenez Rezende, M. Welling, Semi-supervised learning with deep generative models, *Advances in neural information processing systems* 27 (2014).
- [49] A. Odena, Semi-supervised learning with generative adversarial networks, *arXiv preprint arXiv:1606.01583* (2016).
- [50] A. Oliver, A. Odena, C. A. Raffel, E. D. Cubuk, I. Goodfellow, Realistic evaluation of deep semi-supervised learning algorithms, *Advances in neural information processing systems* 31 (2018).
- [51] D. Berthelot, N. Carlini, I. Goodfellow, N. Papernot, A. Oliver, C. A. Raffel, Mixmatch: A holistic approach to semi-supervised learning, *Advances in neural information processing systems* 32 (2019).
- [52] D.-H. Lee, et al., Pseudo-label: The simple and efficient semi-supervised learning method for deep neural networks, in: Workshop on challenges in representation learning, ICML, volume 3, Atlanta, 2013, p. 896.
- [53] C.-W. Kuo, C.-Y. Ma, J.-B. Huang, Z. Kira, Manifold graph with learned prototypes for semi-supervised image classification, *arXiv preprint arXiv:1906.05202* (2019).
- [54] S. Laine, T. Aila, Temporal ensembling for semi-supervised learning, *arXiv preprint arXiv:1610.02242* (2016).
- [55] A. Tarvainen, H. Valpola, Mean teachers are better role models: Weight-averaged consistency targets improve semi-supervised deep learning results, *Advances in neural information processing systems* 30 (2017).
- [56] B. Athiwaratkun, M. Finzi, P. Izmailov, A. G. Wilson, There are many consistent explanations of unlabeled data: Why you should average,

- arXiv preprint arXiv:1806.05594 (2018).
- [57] Q. Xie, M.-T. Luong, E. Hovy, Q. V. Le, Self-training with noisy student improves imagenet classification, in: Proceedings of the IEEE/CVF conference on computer vision and pattern recognition, 2020, pp. 10687–10698.
 - [58] Y. Grandvalet, Y. Bengio, Semi-supervised learning by entropy minimization, Advances in neural information processing systems 17 (2004).
 - [59] E. Donato, E. Falotico, T. G. Thuruthel, Multi-modal perception for soft robotic interactions using generative models, in: 2024 IEEE 7th International Conference on Soft Robotics (RoboSoft), IEEE, 2024, pp. 311–318.
 - [60] R. P. Babadian, K. Faez, M. Amiri, E. Falotico, Fusion of tactile and visual information in deep learning models for object recognition, Information Fusion 92 (2023) 313–325.
 - [61] T. Baltrušaitis, C. Ahuja, L.-P. Morency, Multimodal machine learning: A survey and taxonomy, IEEE transactions on pattern analysis and machine intelligence 41 (2018) 423–443.
 - [62] J. Ngiam, A. Khosla, M. Kim, J. Nam, H. Lee, A. Y. Ng, Multimodal deep learning, in: Proceedings of the 28th international conference on machine learning (ICML-11), 2011, pp. 689–696.
 - [63] C. Silberer, M. Lapata, Learning grounded meaning representations with autoencoders, in: Proceedings of the 52nd Annual Meeting of the Association for Computational Linguistics (Volume 1: Long Papers), 2014, pp. 721–732.
 - [64] N. Srivastava, R. Salakhutdinov, Learning representations for multimodal data with deep belief nets, in: International conference on machine learning workshop, volume 79, 2012, pp. 978–1.
 - [65] N. Srivastava, R. R. Salakhutdinov, Multimodal learning with deep boltzmann machines, Advances in neural information processing systems 25 (2012).
 - [66] Y. Kim, H. Lee, E. M. Provost, Deep learning for robust feature generation in audiovisual emotion recognition, in: 2013 IEEE international conference on acoustics, speech and signal processing, IEEE, 2013, pp. 3687–3691.
 - [67] J. Huang, B. Kingsbury, Audio-visual deep learning for noise robust speech recognition, in: 2013 IEEE international conference on acoustics, speech and signal processing, IEEE, 2013, pp. 7596–7599.
 - [68] D. Wu, L. Shao, Multimodal dynamic networks for gesture recognition, in: Proceedings of the 22nd ACM international conference on Multimedia, 2014, pp. 945–948.
 - [69] W. Ouyang, X. Chu, X. Wang, Multi-source deep learning for human pose estimation, in: Proceedings of the IEEE conference on computer vision and pattern recognition, 2014, pp. 2329–2336.
 - [70] A. Frome, G. S. Corrado, J. Shlens, S. Bengio, J. Dean, M. Ranzato, T. Mikolov, Devise: A deep visual-semantic embedding model, Advances in neural information processing systems 26 (2013).
 - [71] F. Sarfraz, B. Zonooz, E. Arani, Beyond unimodal learning: The importance of integrating multiple modalities for lifelong learning, arXiv preprint arXiv:2405.02766 (2024).
 - [72] L. Xu, Q. Wu, L. Pan, F. Meng, H. Li, C. He, H. Wang, S. Cheng, Y. Dai, Towards continual egocentric activity recognition: A multimodal egocentric activity dataset for continual learning, IEEE Transactions on Multimedia (2023).
 - [73] E. Kazakos, A. Nagrani, A. Zisserman, D. Damen, Epic-fusion: Audio-visual temporal binding for egocentric action recognition, in: Proceedings of the IEEE/CVF international conference on computer vision, 2019, pp. 5492–5501.
 - [74] J. Achiam, S. Adler, S. Agarwal, L. Ahmad, I. Akkaya, F. L. Aleman, D. Almeida, J. Altenschmidt, S. Altman, S. Anadkat, et al., Gpt-4 technical report, arXiv preprint arXiv:2303.08774 (2023).
 - [75] G. M. Van de Ven, T. Tuytelaars, A. S. Tolias, Three types of incremental learning, Nature Machine Intelligence 4 (2022) 1185–1197.
 - [76] Y. Hao, Z. Gong, Z. Xie, S. Guan, X. Yang, Z. Ren, T. Wang, L. Wen, Universal soft pneumatic robotic gripper with variable effective length (2016) 6109–6114.
 - [77] G. Saggio, F. Riillo, L. Sbernini, L. R. Quitadamo, Resistive flex sensors: a survey, Smart Materials and Structures 25 (2015) 013001.
 - [78] R. B. Mishra, N. El-Atab, A. M. Hussain, M. M. Hussain, Recent progress on flexible capacitive pressure sensors: From design and materials to applications, Advanced materials technologies 6 (2021) 2001023.
 - [79] A. Hollinger, M. M. Wanderley, Evaluation of commercial force-sensing resistors, in: Proceedings of the International Conference on New Interfaces for Musical Expression, Paris, France, Citeseer, 2006, pp. 4–8.
 - [80] J. Smith, J. Balloch, Y.-C. Hsu, Z. Kira, Memory-efficient semi-supervised continual learning: The world is its own replay buffer, in: 2021 International Joint Conference on Neural Networks (IJCNN), IEEE, 2021, pp. 1–8.
 - [81] A. Vaswani, N. Shazeer, N. Parmar, J. Uszkoreit, L. Jones, A. N. Gomez, Ł. Kaiser, I. Polosukhin, Attention is all you need, Advances in neural information processing systems 30 (2017).
 - [82] K. He, X. Zhang, S. Ren, J. Sun, Deep residual learning for image recognition, in: Proceedings of the IEEE conference on computer vision and pattern recognition, 2016, pp. 770–778.
 - [83] O. Russakovsky, J. Deng, H. Su, J. Krause, S. Satheesh, S. Ma, Z. Huang, A. Karpathy, A. Khosla, M. Bernstein, et al., Imagenet large scale visual recognition challenge, International journal of computer vision 115 (2015) 211–252.
 - [84] T. Akiba, S. Sano, T. Yanase, T. Ohta, M. Koyama, Optuna: A next-generation hyperparameter optimization framework, in: Proceedings of the 25th ACM SIGKDD international conference on knowledge discovery & data mining, 2019, pp. 2623–2631.
 - [85] E. Broadbent, M. Billingham, S. G. Boardman, P. M. Doraiswamy, Enhancing social connectedness with companion robots using ai, Science robotics 8 (2023) eadi6347.
 - [86] S. K. Min, R. Delgado, W. C. Byoung, Comparative study of ros on embedded system for a mobile robot, Journal of Automation, Mobile Robotics and Intelligent Systems (2018) 61–67.